

1 **Title**

2 **MicroRNAs involved in the regulation of LC-PUFA biosynthesis in teleosts: miR-**
3 **33 enhances LC-PUFA biosynthesis in *Siganus canaliculatus* by targeting *insig1***
4 **which in turn up-regulates *srebpl***

5

6 **Authors**

7 Jun Jun Sun ^{1,3}, Li Guo Zheng¹, Cui Ying Chen^{1,3}, Jin Ying Zhang¹, Cui Hong You^{1, 3},
8 Qing Hao Zhang¹, Hong Yu Ma^{1,3}, Óscar Monroig ⁴, Douglas R. Tocher ⁵, Shu Qi Wang
9 ^{1,3*}, Yuan You Li ^{2*}

10

11 **Addresses**

12 ¹ Guangdong Provincial Key Laboratory of Marine Biotechnology, Shantou
13 University, Shantou 515063, China

14 ² School of Marine Sciences, South China Agricultural University, Guangzhou
15 510642, China

16 ³ STU-UMT Joint Shellfish Research Laboratory, Shantou University, Shantou
17 515063, China

18 ⁴ Instituto de Acuicultura Torre de la Sal, Consejo Superior de Investigaciones
19 Científicas (IATS-CSIC), 12595 Ribera de Cabanes, Castellón, Spain

20 ⁵ Institute of Aquaculture, Faculty of Natural Sciences, University of Stirling, Stirling
21 FK9 4LA, Scotland, UK

22

23 ***Corresponding Author**

24 Prof. Yuanyou Li, Ph.D. (E-mail: yyli16@scau.edu.cn; Tel: 020-87571321)

25 Shuqi Wang, Ph.D. (E-mail: sqw@stu.edu.cn; Tel: 0754-86500614)

26

27 **Abstract**

28 Post-transcriptional regulatory mechanisms play important roles in the regulation
29 of LC-PUFA biosynthesis. Our previous study revealed that miR-33 could increase the
30 expression of fatty acyl desaturases (*fads2*) in the rabbitfish *Siganus canaliculatus*, but
31 the specific mechanism is unknown. Here, we confirmed that miR-33 could target the
32 3'UTR of insulin-induced gene 1 (*insig1*), resulting in down-regulation of its protein
33 level in the rabbitfish hepatocyte line (SCHL). *In vitro* overexpression of miR-33
34 inhibited the mRNA level of *insig1* and increased the mRNA levels of $\Delta 6\Delta 5$ *fads2* and
35 *elovl5*, as well as *srebp1*. In SCHL cells, proteolytic activation of sterol-regulatory-
36 element-binding protein-1 (Srebp1) was blocked by Insig1, with overexpression of
37 *insig1* decreasing mature Srebp1 level, while inhibition of *insig1* led to the opposite
38 effect. Srebp1 could enhance the promoter activity of $\Delta 6\Delta 5$ *fads2* and *elovl5*, whose
39 expression levels decreased with knockdown of *srebp1* in SCHL. Overexpression of
40 miR-33 also resulted in a higher conversion of 18:3n-3 to 18:4n-3 and 20:5n-3 to 22:5n-
41 3, linked to desaturation and elongation via $\Delta 6\Delta 5$ Fads2 and Elov15, respectively. The
42 results suggested that the mechanism by which miR-33 regulates LC-PUFA
43 biosynthesis in rabbitfish is through enhancing the expression of *srebp1* by targeting
44 *insig1*. The findings here provide more insight to the mechanism of miRNAs
45 involvement in the regulation of LC-PUFA biosynthesis in teleosts.

46

47 **Key words:** miR-33; *insig1*; *srebp1*; $\Delta 6\Delta 5$ *fads2*; *elovl5*; LC-PUFA biosynthesis

48

49 **1. Introduction**

50 Long-chain ($\geq C_{20}$) polyunsaturated fatty acids (LC-PUFA) are highly bioactive
51 forms of PUFA. The LC-PUFA with crucial physiological functions in humans and
52 other animals (Janssen and Kiliaan 2014; Calder 2015) include arachidonic acid (ARA;
53 20:4n-6), eicosapentaenoic acid (EPA; 20:5n-3) and docosahexaenoic acid (DHA;
54 22:6n-3). As important components of cell membranes, LC-PUFA reduce membrane
55 phase-change temperatures and enhance membrane fluidity, as well as playing crucial
56 roles in maintaining the normal physiological function of biofilms (Xiao et al. 2001).
57 LC-PUFA are also important in growth, survival, pigmentation, stress and disease
58 resistance of fish, as well as in the development of brain, vision and the nervous system
59 (Sargent et al. 2002; Tocher 2010).

60 The biosynthesis of LC-PUFA involves desaturation and chain elongation reactions
61 that convert the C_{18} PUFA precursors, linoleic acid (LA; 18:2n-6) and α -linolenic acid
62 (ALA; 18:3n-3), into the physiologically important ARA, EPA and DHA. Fish are
63 important sources of n-3 LC-PUFA in the human diet and, consequently, LC-PUFA
64 biosynthesis in fish has been investigated extensively in recent years (Castro et al. 2016;
65 Monroig et al. 2018). Generally, freshwater fish have the ability to convert LA and ALA
66 to C_{20-22} LC-PUFA (ARA, EPA and DHA), with this process requiring enzymes such as
67 fatty acyl desaturases (Fads) and elongation of very-long-chain fatty acids (Elovl)
68 proteins. Fads and Elovl enzymes involved in LC-PUFA biosynthesis can also be found
69 in marine fish, but lower activity and/or absence of key enzymatic capacities is
70 associated with low LC-PUFA biosynthesizing capacity and thus dietary provision of

71 EPA and DHA is required to sustain growth and development (Tocher et al. 2003). The
72 rabbitfish *Siganus canaliculatus* is an exception to this pattern since this marine
73 herbivore has the ability to biosynthesize LC-PUFA from C₁₈ PUFA (Li et al. 2010;
74 Monroig et al. 2012). *S. canaliculatus*, in addition to its complement of elongases
75 (Monroig et al. 2012), possesses two distinct *fads2* genes encoding $\Delta 6\Delta 5$ and $\Delta 4$
76 desaturases enabling all desaturation reactions involved in the LC-PUFA biosynthesis
77 pathway (Castro et al. 2016; Monroig et al. 2018). Consequently, *S. canaliculatus* and
78 has become a valuable model for studying regulatory mechanisms of LC-PUFA
79 biosynthesis in teleosts (Li et al. 2010; Monroig et al. 2012).

80 MicroRNAs (miRNAs) are a class of highly conserved, small non-coding, ~22
81 nucleotides (nt) RNA molecules that are widespread in organisms. In land animals,
82 miRNAs generally exhibit a negative regulatory effect on gene expression and are
83 involved in a number of biological processes (Alvarezgarcia and Miska 2005;
84 Carrington et al. 2003; Xu et al. 2003). Post-transcriptional regulatory mechanisms
85 have been shown to play important roles in LC-PUFA biosynthesis and glycolipid
86 metabolism, as well as growth, development, reproduction and immune function in
87 teleosts (Gong et al. 2015; Her et al. 2011; Siddique et al. 2016; Škugor et al. 2014; Tao
88 et al. 2018; Zhang et al. 2014; Zhu et al. 2015). In rabbitfish, miR-17 was found to be
89 involved in the regulation of LC-PUFA biosynthesis by targeting $\Delta 4 fads2$ (Zhang et al.
90 2014). Moreover, our previous study revealed that miR-33 was involved in the
91 regulation of LC-PUFA biosynthesis by increasing the expression of *fads2* in rabbitfish
92 (Zhang et al. 2016b), although the underlying mechanism was not clearly established.

93 In mammals, miR-33 exists as two distinct isoforms, namely miR-33a and b, which
94 differ from each other in two bases outside the seed region of the mature versions
95 (Najafi-Shoushtari et al. 2010). Both miR-33a and miR-33b are located in the sterol
96 regulatory element-binding protein (*SREBP*) intron region (Najafi-Shoushtari et al.
97 2010; Rayner et al. 2010; Goldstein et al. 2002). In rabbitfish, the miR-33 gene was
98 identified within intron 16 of the gene encoding *srebp1*, and miR-33 overexpression
99 suppressed the expression of *insig1*, which is predicted to be the target gene of miR-33
100 (Zhang et al. 2016b). However, whether this is a direct effect or not is unclear. Moreover,
101 miR-33 overexpression led to an increase in the mRNA levels of *fads2* and *srebp1* and,
102 thus, it is believed to be involved in the regulation of LC-PUFA biosynthesis, but the
103 specific mechanism is unknown (Zhang et al. 2016b).

104 The Insulin-induced gene protein (Insig) is an important factor in the regulation of
105 lipid metabolism (Jo et al. 2011). The two subtypes of Insig, namely Insig1
106 (Radhakrishnan et al. 2007) and Insig2 (Lee et al. 2005), combine with Srebp and Srebp
107 cleavage activating protein (SCAP) in the endoplasmic reticulum (ER) as an Insig-
108 SCAP-Srebp complex. Insig1 has a stronger affinity for SCAP compared to Insig2, and
109 is reported to block the proteolytic cleavage of Srebp proteins by retaining Srebp
110 precursors in the ER membrane, consequently decreasing lipogenesis (Gong et al. 2006;
111 Engelking et al. 2004). In particular, the mechanisms detailed above apply to mammals,
112 and it remains unclear whether Insig1 can block Srebp proteolytic activation in teleost
113 fish.

114 In mammals, miR-33 has been found within the intron of *srebp* genes and reported

115 to function in cooperation with its host (Horie et al. 2013). *Srebp1* is an important
116 transcription factor involved in regulating the expression of key enzymes in LC-PUFA
117 synthesis in liver (Nara et al. 2002; CarmonaAntoñanzas et al. 2014). *Srebp1* affects
118 the synthesis of LC-PUFA via activation of acetyl CoA carboxylase (ACC), fatty acid
119 synthetase (FAS), stearoyl-CoA desaturase (SCD) and other enzymes related to fatty
120 acid metabolism in mouse liver (Shimomura et al. 1998). *Srebp1c* is also reported to
121 promote the expression of $\Delta 5$ and $\Delta 6$ *fads-like* genes in the liver (Qin et al. 2009). In
122 rabbitfish, our previous studies showed there might be potential interaction between
123 *Srebp1* and the key enzymes of LC-PUFA synthesis, especially $\Delta 6\Delta 5$ *Fads2* and the
124 PUFA elongase, *Elovl5*, and the sterol regulatory element (SRE) of *Srebp* protein
125 predicted in the promoter region of $\Delta 6\Delta 5$ *fads2* and *elovl5* (Zhang et al. 2016; Dong et
126 al. 2018).

127 The aim of the present study was to investigate the mechanism underpinning the
128 regulation of LC-PUFA biosynthesis by miR-33. Firstly, dual luciferase assay and
129 western blotting were performed to determine whether *insig1* was a direct target gene
130 of miR-33. Secondly, to explore the functional relationship between *Insig1* and *Srebp1*
131 in rabbitfish, overexpression and inhibition of *insig1* followed by western blotting was
132 used to detect the protein abundances of *Insig1* and mature *Srebp1*. Subsequently, in
133 order to further elucidate the roles of *Srebp1* in the regulation of LC-PUFA biosynthesis
134 in rabbitfish, changes in the expression, as well as the promoter activity, of $\Delta 6\Delta 5$ *fads2*
135 and *elovl5*, in response to changes in the *in vitro* expression level of *srebp1* were
136 explored. The data provide the basis for elucidating the mechanism of miR-33

137 involvement in the regulation of LC-PUFA biosynthesis in rabbitfish, as well as
138 providing the theoretical basis for the participation of miRNA in the regulation of LC-
139 PUFA biosynthesis in teleosts.

140

141 **2. Materials & Methods**

142 **2.1 Rabbitfish hepatocyte culture**

143 The rabbitfish *S. canaliculatus* hepatocyte line (SCHL) was successfully
144 established in our laboratory (Liu et al. 2017) SCHL cell line was cultured at 28 °C in
145 Dulbecco's modified Eagle's medium/nutrient F12 (DMEM/F12, Gibco, Life
146 Technologies, USA) containing 20 mM 4-(2-hydroxyethyl) piperazine-1-
147 ethanesulphonic acid (HEPES, Sigma-Aldrich, USA), 10 % fetal bovine serum (FBS,
148 Gibco, Life Technologies, USA), 0.5 % rainbow trout *Oncorhynchus mykiss* serum
149 (Caisson Labs), penicillin (100 U ml⁻¹, Sigma-Aldrich, USA) and streptomycin (100 U
150 ml⁻¹, Sigma-Aldrich, USA).

151

152 **2.2 Plasmid construction**

153 In order to achieve overexpression of *insig1*, we constructed the pcDNA-Insig1
154 eukaryotic expression vector at the *EcoRI* and *XhoI* (New England Biolabs, Ipswich,
155 USA) restriction sites, with full-length sequence of *insig1* amplified using pcDNA-
156 Insig1-F/R primers (Table 1). Similarly, we constructed the pcDNA3.1-SREBP
157 overexpression vector at the *XbaI* and *HindIII* restriction sites, with full-length
158 sequence of *srebpl* amplified using LG-SREBP-F/R primers (Table 1). The *Δ6Δ5 fads2*

159 and *elovl5* promoter deletion dual luciferase reporter vectors were constructed
160 previously in our laboratory (Dong et al., 2018). For heterologous expression of
161 rabbitfish miR-33, a DNA fragment encompassing rabbitfish pre-miR-33 was digested
162 with *EcoRI* and *BamHI* and inserted into the pEGFP-C3 plasmid. To construct the dual
163 luciferase reporter vectors, DNA fragments were inserted into pmirGLO dual-luciferase
164 miRNA target expression vector (Promega, Madison, WI, USA) at the *SacI* and *XbaI*
165 restriction sites. The recombinant vectors were: (1) pmirGLO-Insig-3'UTR, pmirGLO
166 including an insert consisting of a partial DNA fragment of the rabbitfish *insig1* 3'UTR,
167 which includes the binding site of miR-33 in rabbitfish, amplified with Insig-3'UTR-
168 F/R primers (Table 1); (2) pmirGLO -Insig-3'UTR-MU, pmirGLO including an insert
169 consisting of the predicted binding site of miR-33 in *insig1* 3'UTR (5'-AATGCA-3')
170 mutated into 5'-TAAGGA-3' to prevent complementarity of miR-33, and amplified
171 with mutation primers Insig-3'UTR-Mu-F/R designed following the instructions of the
172 Muta-direct TM site-Directed Mutagenesis Kit (SBS Genetech Co., Ltd., Beijing,
173 China); (3) pmirGLO-R33 (positive control), pmirGLO including an insert consisting
174 of a synthesized oligonucleotide containing a 100 % match to miR-33 (Sangon Biotech,
175 Shanghai, China). Sequences of primers and oligonucleotides used for cloning are
176 provided in Table 1.

177

178 **2.3 RNA isolation and quantitative real-time PCR (qPCR)**

179 Total RNA was extracted using Trizol reagent (Invitrogen, Carlsbad, CA, USA)
180 followed by determination of the concentration and quality of the total RNA on

181 NanoDrop 2000 (Thermo Scientific, USA). cDNA was synthesized with 1 µg total RNA
182 using the miScript II RT Kit (Qiagen, Hilden, Germany), and the expression of miR-33
183 determined using the miScript SYBR Green PCR Kit (Qiagen, Hilden, Germany) with
184 miR-33 specific primer (qPCR-miR-33) (Table 1) and universal primers. For the qPCR
185 determination of the mRNA expression levels of *insig1* (KU598855), *srebpl*
186 (JF502069.1), *Δ6Δ5 fads2* (EF424276.2) and *elovl5* (GU597350.1), LightCycler® 480
187 SYBR Green I Master (Roche, Germany) was used with rabbitfish gene-specific
188 primers (Table 1). The relative RNA level of each gene was normalized to that of 18s
189 rRNA (AB276993), and calculated using the comparative threshold cycle method
190 (Livak and Schmittgen 2012). All reactions were run on LightCycler® 480
191 thermocycler (Roche, Germany) using qPCR programs according to manufacturer's
192 specifications.

193

194 **2.4 Dual-luciferase assay**

195 To determine whether *insig1* was a direct target gene of miR-33, a dual luciferase
196 assay was performed using human embryonic kidney (HEK 293T) cells (Chinese Type
197 Culture Collection, Shanghai, China). The HEK 293T cells were seeded into 96-well
198 cell culture plates in 100 µl High Glucose Dulbecco's Modified Eagle Medium (DMEM)
199 (Gluta MAX) (Gibco, Life Technologies, USA) with 10 % fetal bovine serum per well
200 (FBS, Sijiqing Biological Engineering Material Company, China). The HEK 293T cells
201 were grown for 24 h to 80 % confluence, and then co-transfected with either pEGFP-
202 miR-33 (50 ng) or pEGFP-empty (50 ng) with different recombinant dual luciferase

203 reporter vectors (50 ng) using Lipofectamine[®] 2000 Reagent (Invitrogen, Carlsbad,
204 USA) according to the manufacturer's instructions. Firefly and Renilla luciferase
205 activities were quantified after 48 h transfection using a microplate reader (Infinite
206 M200 Pro, Tecan, Switzerland) and firefly luciferase activity was normalized to Renilla
207 luciferase activity. Eight replicate wells were used for each treatment.

208

209 **2.5 Western blotting**

210 In order to further study the potential relationship between miR-33 and the target
211 gene *Insig1* at the protein level, Western blotting was carried out. miR-33 was up-
212 regulated by transfection with miR-33 mimics (dsRNA oligonucleotides) and negative
213 control (NC) oligonucleotides were obtained from Genepharma (Shanghai, China). The
214 sequences were as follows: miR-33 mimic, sense, 5'-
215 CGUGCAUUGUAGUUGCAUUG-3'; antisense, 5'-
216 AUGCAACUACAAUGCACGUU -3'. SCHL cells were seeded onto 100 mm plates
217 (2×10^6 cells per plate), grown for 24 h to 80 % confluence, and then transfected with
218 300 pmol miR-33 mimics or NC using Lipofectamine[®] 2000 Reagent, in triplicate.
219 Total protein was extracted at 48 h post-transfection using cell total protein extraction
220 kit (Sangon Biotech, Shanghai, China) and concentrations quantified with non-
221 interference protein assay kit (Sangon Biotech, Shanghai, China). Next, 30 μ L of each
222 sample was loaded and separated on a 12 % SDS/PAGE, transferred onto PVDF
223 membranes, and then incubated with anti-*Insig1* rabbit pAb (Wanleibio, Shenyang,
224 China) at 1:500 dilution. Actin level, determined using anti-actin antibody (Beyotime,

225 Haimen, China) at 1:2000 dilution, was used for normalization. After three washes with
226 Tris-Buffered Saline Tween (TBST), membranes were incubated with goat-anti-rabbit
227 and goat-anti-mouse (Millipore, Bedford, MA, USA) secondary antibodies at a ratio of
228 1:15000. Membranes were washed three times with TBST, and the immunoreactive
229 bands visualized using the Odyssey infrared imaging system 2.1 (LI-COR, USA), and
230 analyzed by Image studio (ver 5.2) software with the quantity of *Insig1* and Actin
231 protein converted into intensity values.

232

233 **2.6 Overexpression of miR-33 to investigate the functional relationship between** 234 **miR-33 and LC-PUFA biosynthesis-related genes**

235 To further investigate the potential role of miR-33 in the regulation of gene
236 expression in LC-PUFA biosynthesis, miR-33 was up-regulated by transfection with
237 miR-33 mimics. SCHL cells were seeded into six-well plate (5×10^5 cells per well),
238 grown for 24 h to 80 % confluence, and then transfected with 100 pmol miRNA mimics
239 or NC with Lipofectamine[®] 2000 Reagent, each process consisting of six replicates. At
240 24 h post transfection, SCHL cells were harvested, RNA extracted and subjected to
241 qPCR analysis of expression levels of *insig1*, *srebp1*, *Δ6Δ5 fads2* and *elovl5* mRNA.

242

243 **2.7 Overexpression and inhibition of *insig1* to explore the functional relationship** 244 **between *Insig1* and *Srebp1***

245 SCHL cells were seeded onto 100 mm plates (2×10^6 cells per plate), grown for 24
246 h to 80 % confluence, and then transfected with 4 μg pcDNA-*Insig1* overexpression

247 plasmid using X-tremeGENE HP DNA Transfection Reagent (Roche, Germany), in
248 triplicate. Silencing of *insig1* expression was performed using small interfering RNA
249 (siRNA) duplexes obtained from Ribobio (Guangzhou, China) with the following
250 sequences: si-*insig1* sense, 5'-CAAAGCUGAAGAAAUGAUdTdT-3'; si-*insig1*
251 antisense, 5'-AUCAUUUCUUCAGCUUUGGdTdT-3', and SCHL transfected with 50
252 nM of each siRNA. The *insig1*-specific siRNA (si-*insig1*) or negative control (si-NC)
253 was performed with Lipofectamine[®] 2000 Reagent. The cells were harvested at 48 h
254 post transfection and subsequently subjected to Western blotting analysis as described
255 above. In addition, the anti-Srebp1 rabbit pAb was purchased from Wanleibio
256 (Shenyang, China) and used as a dilution of 1:500.

257

258 **2.8 Promoter analysis to explore the functional relationship between *srebp1*, $\Delta 6\Delta 5$** 259 ***fads2* and *elovl5***

260 To investigate the functional relationship between *srebp1* and the promoters of
261 $\Delta 6\Delta 5$ *fads2* and *elovl5*, a dual luciferase assay was performed. The relationship between
262 these constructs was investigated using HEK 293T cells, which were co-transfected
263 with 100 ng pcDNA3.1-SREBP eukaryotic expression vector and 50 ng $\Delta 6\Delta 5$ *fads2* or
264 *elovl5* promoter deletion dual luciferase reporter vectors with Lipofectamine[®] 2000
265 Reagent (Invitrogen, Carlsbad, CA, USA). The Renilla reporter vector pGL4.75
266 plasmid was used as the internal reference. Firefly and Renilla luciferase activities were
267 quantified after 48 h transfection by a microplate reader (Infinite M200 Pro, Tecan,
268 Switzerland) and firefly luciferase activity was normalized to Renilla luciferase activity.

269

270 **2.9 Inhibition of *srebp1* in rabbitfish hepatocytes**

271 For *srebp1* RNAi in SCHL cells, three pairs of siRNAs, namely siRNA-638,
272 siRNA-1211 and siRNA-1303, were designed (numbers represented the location of the
273 target site of the siRNA on the gene) and synthesized by a commercial company
274 (Genepharma, Shanghai, China). SCHL cells were seeded onto six-well plates with $5 \times$
275 10^5 cells per well, grown for 24 h to 80 % confluence, and then transfected with the
276 siRNAs or NC using the RNAiMAX Reagent (Invitrogen, Carlsbad, CA, USA) in
277 triplicate. At 48 h post transfection, SCHL cells were harvested, RNA extracted and
278 subjected to qPCR determination of the mRNA expression levels of *srebp1*.

279

280 **2.10 Fatty acid analysis**

281 SCHL cells were seeded onto 100 mm plates at a density of 2×10^6 cells per plate,
282 grown for 24 h to 80 % confluence, and then transfected with 300 pmol miRNA mimics
283 or NC with Lipofectamine[®] 2000 Reagent triplicates. After 48h incubation, cells were
284 harvested for fatty acid composition analysis by gas chromatography (GC) after
285 chloroform/methanol extraction, saponification and methylation with boron trifluoride
286 (Sigma-Aldrich, USA) as described previously (Li et al., 2010; Chen et al., 2016). For
287 identification, the retention times of the fatty acids were compared to those of standard
288 methyl esters (Sigma-Aldrich, USA), with quantification of each fatty acid in a certain
289 number of cells being estimated using the signal of the internal standard 17:0
290 (heptadecanoic acid) (Sigma-Aldrich, USA). Fatty acid contents were expressed as

291 percentage of total fatty acids (Table 2).

292

293 **2.11 Statistical analysis**

294 All the data are presented as means \pm SEM. The dual-luciferase assay and qPCR
295 expression data were analyzed by one-way analysis of variance (ANOVA) followed by
296 Tukey's multiple comparison test or Student's t-test using Origin 7.0. A significance of
297 $P < 0.05$ was applied to all statistical tests performed.

298

299 **3. Results**

300 **3.1 miR-33 targets to the 3'UTR of *insig1***

301 Bioinformatic analyses showed that potential binding sites of *S. canaliculatus* miR-
302 33 (sca-miR-33) were found in the 3'UTR of *insig1* in rabbitfish (Fig. 1a) (Zhang et al.,
303 2016). Based on this, a dual luciferase assay was used to further verify the interaction
304 between miR-33 and *insig1*. Results from the qPCR analysis revealed that HEK 293T
305 cells transfected with pEGFP-miR-33 had a 140-fold higher level of rabbitfish miR-33
306 expression than the endogenous background of miR-33 ($P < 0.01$) (Fig. 1b). The results
307 of the dual luciferase reporter assay showed that: i) in negative control groups, there
308 was no difference between the pEGFP-empty /pmirGLO-empty co-transfected group
309 (Fig. 1c: lane 1) and the pEGFP-miR-33/pmirGLO-empty co-transfected group (Fig.
310 1c: lane 2); ii) in positive control groups, the pEGFP-miR-33/pmirGLO-R33 co-
311 transfected group (Fig. 1c: lane 4) showed significantly lower normalized Luc activity
312 than the pEGFP-empty/pmirGLO-R33 group (Fig. 1c: lane 3) ($P < 0.01$). If the

313 heterologous expression of miRNA interacts with the inserted target fragment, the Luc
314 activity would decrease and, therefore, this result proved that the dual luciferase assay
315 report system worked well; iii) in the experimental groups (Fig. 1c: lanes 5-8), the
316 pEGFP-miR-33/pmirGLO-Insig-3'UTR co-transfected group (Fig. 1c: lane 6) showed
317 significantly lower normalized Luc activity than the pEGFP-empty/pmirGLO-Insig-
318 3'UTR group ($P < 0.05$) (Fig. 1c: lanes 5). However, when a mutation is introduced
319 into the predicted binding sites of miR-33 at 3'UTR of *insig1* mRNA, the inhibition
320 was eliminated (Fig. 1c: lanes 7-8).

321

322 **3.2 Overexpression of miR-33 inhibits the activity of Insig1 protein in SCHL**

323 Western blotting was used to further study the potential relationship between miR-
324 33 and its target protein Insig1. After overexpression of miR-33, the protein level of
325 Insig1 decreased by 40 % compared with the NC group (Fig. 2). It was observed that
326 miR-33 had an inverse expression pattern with Insig1 protein level in rabbitfish.

327

328 **3.3 Overexpression of miR-33 impacts on *insig1* expression inducing *srebpl* 329 *downstream genes including $\Delta 6\Delta 5$ *fads2* and *elovl5****

330 To further investigate the potential role of miR-33 in regulating the expression of
331 genes involved in LC-PUFA biosynthesis, miR-33 was overexpressed by transfection
332 with miR-33 mimics. At 24 h post-treatment, the expression of *insig1* was inhibited
333 whereas the expression of *srebpl* and $\Delta 6\Delta 5$ *fads2* and *elovl5* were up-regulated, with
334 the expression of *elovl5* significantly increased ($P < 0.05$) (Fig. 3).

335

336 **3.4 Insig1 can block the formation of mature Srebp1 protein in rabbitfish**
337 **hepatocytes**

338 In order to provide direct proof for Insig1 being able to block Srebp proteolytic
339 activation, Western blotting was used to further study the potential relationship between
340 Insig1 and Srebp1. The protein levels of mature Srebp1 and Insig1 were detected after
341 overexpression and inhibition of *insig1*. With overexpression of *insig1*, the protein level
342 of Insig1 increased by 1.5-fold, while the protein level of mature Srebp1 decreased by
343 50 % compared with the pcDNA3.1 group (Fig. 4a). With inhibition of *insig1*, the
344 protein level of Insig1 decreased by 30 %, while the protein level of mature Srebp1
345 increased by 1.5-fold compared with the si-NC group (Fig. 4b).

346

347 **3.5 Functional relationship between *srebp1* and $\Delta 6\Delta 5$ *fads2* and *elovl5*.**

348 Our previous studies predicted that the SRE binding element of Srebp protein was
349 present in the promoter regions of $\Delta 6\Delta 5$ *fads2* and *elovl5* in rabbitfish (Fig. 5) (Dong et
350 al., 2018). Thus, the pcDNA3.1-SREBP eukaryotic expression plasmid, $\Delta 6\Delta 5$ *fads2* and
351 *elovl5* promoter deletion dual luciferase reporter vectors were co-transfected into HEK
352 293T cells. The dual luciferase reporter assay results showed that overexpression of
353 *srebp1* resulted in significantly increased fluorescence activity of $\Delta 6\Delta 5$ *fads2* promoter
354 deletion D2 and D4 ($P < 0.05$ and $P < 0.01$), while the fluorescence activity of D1 and
355 D3 was not significantly different from the control group ($P > 0.05$) (Fig. 6). At the
356 same time, when *srebp1* was overexpressed, the fluorescence activity of *elovl5*

357 promoter deletion D1, D2 and D3 significantly increased ($P < 0.05$) (Fig. 7).

358

359 **3.6 *Srebp1* regulates the expression of *Δ6Δ5 fads2* and *elovl5***

360 In order to knockdown *srebp1*, the silencing efficiency of three pairs of siRNA,
361 namely siRNA-638, siRNA-1211 and siRNA-1303, were determined. The results
362 showed that siRNA-638 and siRNA-1211 had significant knockdown effects on *srebp1*
363 mRNA expression ($P < 0.05$) (Fig. 8), with about 16 % and 18 % knockdown efficiency,
364 respectively, while there was no significant difference between siRNA-1303 and the
365 control group ($P > 0.05$). Thus, siRNA-1211 was used for the RNAi experiments.
366 Following successful *srebp1* knockdown with siRNA-1211 in SCHL cells, the
367 expression levels of *Δ6Δ5 fads2* and *elovl5* were also significantly decreased ($P < 0.05$)
368 (Fig. 9).

369

370 **3.7 Up-regulation of miR-33 and biosynthesis of LC-PUFA in rabbitfish** 371 **hepatocytes**

372 The effects of miR-33 on LC-PUFA biosynthesis in SCHL cells was assessed by
373 determining the effects of overexpressing miR-33 on fatty acid composition. It was
374 observed that miR-33 overexpression resulted in a higher conversion of 18:3n-3 to
375 18:4n-3, and 20:5n-3 to 22:5n-3, as well as higher levels of ARA, EPA and DHA in
376 rabbitfish hepatocytes. Compared with the NC group, the conversion of 18:3n-3 to
377 18:4n-3 increasing significantly ($P < 0.05$) (Table 2).

378

379 **4. Discussion**

380 miR-33 is highly conserved in animals and plays a crucial role in the regulation of
381 lipid metabolism, such as reverse cholesterol transport and fatty acid oxidation (Gerin
382 et al. 2010; Horie et al. 2010; Najafi-Shoushtari et al. 2010; Rayner et al. 2010). We
383 reported previously that miR-33 has a potential role in the regulation of LC-PUFA
384 biosynthesis in fish (Zhang et al. 2016b). Hence, the present study aimed to further
385 explore the mechanisms underpinning this finding. In our previous research, we found
386 that overexpression of miR-33 up-regulated the transcription of *Δ4 fads2* and *Δ6Δ5*
387 *fads2*, but suppressed the expression of *insig1*. In mammals, INSIG1 could bind to the
388 sterol-sensing domain of SCAP (SREBP cleavage activating protein), which makes the
389 SCAP/SREBP complex reside longer in the ER, ultimately blocking SREBP entry into
390 the nucleus and preventing its action as a transcription factor (Gong et al. 2006;
391 Engelking et al. 2004). Accordingly, it was necessary to demonstrate the direct effect
392 of miR-33 on *insig1*, including whether *Insig1* can block *Srebp* proteolytic activation,
393 and whether *Srebp1* directly up-regulates the expression of genes involved in LC-PUFA
394 biosynthesis. We herein report compelling evidence corresponding to each of these
395 points.

396 Our data confirmed that miR-33 down-regulated the protein abundance of *Insig1*
397 in rabbitfish through direct targeting of the 3'UTR of *insig1*. Generally, miRNAs
398 depend on the "seed sequence" to identify and partially combine with the 3'UTR of
399 target genes, thereby inducing target mRNA degradation or inhibiting protein
400 translation, manifested by the reduction of function or activity of target genes. The dual

401 luciferase assay revealed that miR-33 could repress the 3'UTR luciferase activity of
402 *insig1*, which provided evidence that *insig1* was a direct target gene of miR-33. In
403 rabbitfish hepatocytes, the overexpression of miR-33 decreased the protein abundance
404 of Insig1, therefore indicating that a negative regulation of miR-33 occurred at the
405 translational level, in agreement with the general mechanism of animal miRNA (Bartel
406 2009; Pillai et al. 2005).

407 Lowering the protein abundance of Insig1 by miR-33 indirectly increased the level
408 of Srebp1 mature protein because the inhibitory effect of Insig on Srebp activation was
409 reduced. Our previous studies showed that, in SCHL cells, miR-24 enhanced the
410 expression of *srebp1* mRNA and the production of mature Srebp1 protein by targeting
411 *insig1*, while opposite results were observed with knockdown of miR-24 in rabbitfish
412 hepatocytes suggesting that *insig1* may inhibit the formation of mature Srebp1 (Chen
413 et al. 2019). In the present study, we confirmed Insig1 can block Srebp proteolytic
414 activation, with overexpression of *insig1* decreasing abundance of mature Srebp1
415 protein, while inhibition of *insig1* leads to an increase in abundance of mature Srebp1
416 protein. This suggested that Insig proteins dissociated from the Insig-SCAP-SREBP
417 complex, so that the SCAP-SREBP complex could transfer to the Golgi (Gong et al.
418 2006; Engelking et al. 2004). It is reported that, under the shear processing of S1P and
419 S2P, the mature protein of Srebp1 is formed, which then enters the nucleus and exerts
420 its regulatory functions (Yang et al. 2002; Yabe et al. 2003). In rabbitfish hepatocytes,
421 overexpression of miR-33 decreased the protein abundance of Insig1, coupled with
422 decreased mRNA expression of *insig1* and increased expression of *srebp1* mRNA. With

423 an increase in the mRNA expression level of *srebp1*, there would be a corresponding
424 increase in the protein abundance of Srebp1. It is known that miR-33 is found within
425 an intron of the *srebp* gene in both mammals and teleosts (Horie et al. 2013; Zhang et
426 al. 2016). In rabbitfish, increased transcription of *srebp1* elevated the abundance of
427 miR-33 in primary hepatocytes (Zhang et al. 2016b). This was interesting as it suggests
428 that transcription of *srebp1* helps to bring about self-proteolysis. In addition, it was
429 observed in the present study that, when miR-33 was overexpressed, the level of *srebp1*
430 also increased. The question here is, how did miR-33 enhance the expression of *srebp1*
431 to participate in LC-PUFA biosynthesis? Research in mice has shown that *srebp1c* can
432 promote the expression of the $\Delta 5$ and $\Delta 6$ *fads-like* genes (Qin et al. 2009). Similarly, it
433 has been reported that Srebp1 can be activated by TO901317, a liver X receptor (*lxr*)
434 agonist, that activates the Lxr-Srebp1 pathway, and further promotes the expression of
435 $\Delta 5$ and $\Delta 6$ *fads* in Atlantic salmon (*Salmo salar*) (Minghetti et al. 2011). Studies have
436 also found that SRE elements are present in the human *FADS2* ($\Delta 6$) promoter (Nara et
437 al. 2002). In Atlantic salmon, Atlantic cod (*Gadus morhua* L.) and zebrafish (*Danio*
438 *rerio*), SRE elements have been predicted in the *\Delta 6 fads2* promoter (Zheng et al. 2009).
439 In rabbitfish, our previous studies characterized the upstream promoter sequences of
440 *\Delta 6\Delta 5 fads2* and *elovl5* genes (Dong et al. 2018) and predicted SRE elements in the
441 upstream promoter sequences. These data indicated that *srebp1* might participate in the
442 regulation of LC-PUFA biosynthesis by regulating *\Delta 6\Delta 5 fads2* and *elovl5*. When further
443 exploring the functional relationship between *srebp1* and the promoters of *\Delta 6\Delta 5 fads2*
444 and *elovl5*, dual luciferase reporter assays showed that overexpression of *srebp1*

445 significantly enhanced the fluorescence activity of $\Delta 6\Delta 5$ *fads2* and *elovl5* promoter
446 containing SRE element. These results demonstrated that *srebp1* can activate the
447 expression of the rabbitfish $\Delta 6\Delta 5$ *fads2* and *elovl5* depending on the SRE element. We
448 previously revealed that *lxr* agonist (TO901317) could significantly increase the mRNA
449 expression level of *srebp1*, together with an increase in the expression of *fads2* in
450 rabbitfish (Zhang et al. 2016a). Here, when the expression of *srebp1* was depleted by
451 RNAi, the expression levels of $\Delta 6\Delta 5$ *fads2* and *elovl5* also decreased. Therefore, miR-
452 33 enhances LC-PUFA biosynthesis by up-regulating *srebp1*, which acting on $\Delta 6\Delta 5$
453 *fads2* and *elovl5* in rabbitfish.

454 Analysis of the differences in the fatty acid composition reflects the ability of C₁₈
455 PUFA to be converted into LC-PUFA through the desaturation and elongation pathway
456 (Brown 2005). We observed that overexpression of miR-33 resulted in higher
457 production of C₂₀₋₂₂ LC-PUFA compared to the NC group, as the level of ARA, EPA
458 and DHA increased in rabbitfish hepatocytes. These findings indicated that miR-33
459 promoted LC-PUFA biosynthesis. Moreover, overexpression of miR-33 increased the
460 conversion of 18:3n-3 to 18:4n-3 and 20:5n-3 to 22:5n-3. Specifically for rabbitfish,
461 the conversion of 18:3n-3 to 18:4n-3 requires the action of the $\Delta 6\Delta 5$ Fads2, while the
462 conversion of 20:5n-3 to 22:5n-3 requires that of Elov15, hence, these results suggested
463 an increase in the enzymatic activities of $\Delta 6/\Delta 5$ Fads2 and Elov15. These results have
464 therefore shown that miR-33 promotes LC-PUFA biosynthesis at the physiological
465 level, which might be achieved by regulating the $\Delta 6\Delta 5$ Fads2 and Elov15, key enzymes
466 in LC-PUFA biosynthesis.

467 In summary, we propose a putative mechanism (Fig. 10), suggesting that miR-33
468 inhibits the translation of Insig1 protein, thereby indirectly increasing the level of
469 mature Srebp1 protein. Since Srebp1 upregulates the expression of key enzymes in LC-
470 PUFA biosynthesis (i.e. $\Delta 6\Delta 5$ Fads2 and Elovl5), so miR-33 can increase the activity
471 of LC-PUFA biosynthesis in rabbitfish. As miR-33 is expressed with transcription of
472 *srebp1*, the interaction between Srebp1 and miR-33 might be a self-promoting
473 mechanism, which helps to enhance the function of Srebp1.

474

475 **Acknowledgements**

476 This work was financially supported by the National Key R&D Program of China
477 (2018YFD0900400), National Natural Science Foundation of China (No. 31873040 &
478 No. 31702357), Natural Science Foundation of Guangdong Province
479 (2018A030313910), China Agriculture Research System (CARS-47) and Innovation
480 and Strong School Projects in Guangdong Province (2016KTSCX037).

481

482 **Compliance with Ethical Standards**

483 **Conflict of Interest** The authors declare that they have no conflict of interest.

484

485 **References**

- 486 Alvarezgarcia I, Miska EA (2005) MicroRNA functions in animal development and
487 human disease. *Development* 132(21): 4653-4662.
488 Bartel DP (2009) MicroRNAs: target recognition and regulatory functions. *Cell* 136 (2):
489 215-33

490 Brown JE (2005) A critical review of methods used to estimate linoleic acid $\Delta 6$ -
491 desaturation ex vivo and in vivo. *Eur J Lipid Sci Tech* 107(2): 119-134.

492 Calder PC (2015) Very long chain omega-3 (n-3) fatty acids and human health. *Eur J*
493 *Lipid Sci Tech* 116(10): 1280-1300.

494 CarmonaAntoñanzas Greta, Tocher DR, Martinezrubio L, Leaver M (2014)
495 Conservation of lipid metabolic gene transcriptional regulatory networks in fish
496 and mammals. *Gene* 534(1): 1-9.

497 Carrington JC, Ambros V (2003) Role of microRNAs in plant and animal development.
498 *Science* 301(5631): 336-338.

499 Castro LF, Tocher DR, Monroig Ó (2016) Long-chain polyunsaturated fatty acid
500 biosynthesis in chordates: insights into the evolution of fads and elovl gene
501 repertoire. *Prog Lipid Res* 62(6): 25-40.

502 Chen CY, Sun BL, Guan WT, Bi YZ, Li PY, Ma J, Chen F, Pan Q, Xie QM (2016) N-3
503 essential fatty acids in Nile tilapia, *Oreochromis niloticus*: effects of linolenic acid
504 on non-specific immunity and anti-inflammatory responses in juvenile fish.
505 *Aquaculture* 450: 250-257.

506 Chen CY, Wang SQ, Zhang M, Chen BJ, You CH, Xie DZ, Liu Y, Zhang QH, Zhang
507 JY, Monroig Ó, Tocher DR, Waiho K, Li YY (2019) miR-24 is involved in
508 vertebrate LC-PUFA biosynthesis as demonstrated in marine teleost *siganus*
509 *canaliculatus*. *BBA-Mol Cell Biol L* 1864(5): 619.

510 Dong YW, Zhao JH, Chen JL, Wang SQ, Liu Y, Zhang QH, You CH, Monroig Ó, Tocher
511 DR, Li YY (2018) Cloning and characterization of $\Delta 6/\Delta 5$ fatty acyl desaturase (fad)
512 gene promoter in the marine teleost *Siganus canaliculatus*. *Gene* 647: 174-180.

513 Engelking LJ, Kuriyama H, Hammer RE, Horton JD, Brown MS, Goldstein JL, Liang
514 G (2004) Overexpression of insig-1 in the livers of transgenic mice inhibits srebp
515 processing and reduces insulin-stimulated lipogenesis. *J Clin Invest* 113(8): 1168-
516 75.

517 Gerin I, Bommer GT, Mccoin CS, Sousa KM, Krishnan V, Macdougald OA (2010)
518 Roles for miRNA-378/378* in adipocyte gene expression and lipogenesis. *Am J*
519 *Physiol-endoc M* 299(2): E198.

520 Gerin I, Clerbaux LA, Haumont O, Lanthier N, Das AK, Burant CF, Leclercq IA,
521 MacDougald OA, Bommer GT (2010) Expression of miR-33 from an srebp2 intron
522 inhibits cholesterol export and fatty acid oxidation. *J Biol Chem* 285(44): 33652.

523 Goldstein JL, Rawson RB, Brown MS (2002) Mutant mammalian cells as tools to
524 delineate the sterol regulatory element-binding protein pathway for feedback
525 regulation of lipid synthesis. *Arch Biochem Biophys* 397(2): 139-148.

526 Gong GY, Sha ZX, Chen SL, Li C, Yan H, Chen YD, Wang TZ (2015) Expression
527 profiling analysis of the microRNA response of *Cynoglossus semilaevis* to *Vibrio*
528 *anguillarum* and other stimuli. *Mar Biotechnol (NY)* 17(3):338-352.

529 Gong Y, Lee JN, Lee PCW, Goldstein JL, Brown MS, Ye J (2006) Sterol-regulated
530 ubiquitination and degradation of insig-1 creates a convergent mechanism for
531 feedback control of cholesterol synthesis and uptake. *Cell Metabolism* 3(1): 15-24.

532 Her GM, Hsu CC, Hong JR, Lai CY, Hsu MC, Pang HW, Chan SK, Pai WY (2011)
533 Overexpression of gankyrin induces liver steatosis in zebrafish (*danio rerio*). *BBA-*
534 *Mol Cell Biol L* 1811(9): 536-548.

535 Horie T, Nishino T, Baba O, Kuwabara Y, Nakao T, Nishiga M, Usami S, Izuhara M,
536 Sowa N, Yahagi N, Shimano H, Matsumura S, Inoue K, Marusawa H, Nakamura
537 T, Hasegawa K, Kume N, Yokode M, Kita T, Kimura T, Ono K (2013) Microrna-
538 33 regulates sterol regulatory element-binding protein 1 expression in mice. *Nature*
539 *Communications* 4(4): 2883.

540 Horie T, Ono K, Horiguchi M, Nishi H, Nakamura T, Nagao K, Kinoshita M, Kuwabara
541 Y, Marusawa H, Iwanaga Y, Hasegawa K, Yokode M, Kimura T, Kita T (2010)
542 Microrna-33 encoded by an intron of sterol regulatory element-binding protein 2
543 (srebp2) regulates hdl in vivo. *P Natl Acad Sci USA* 107(40): 17321-17326.

544 Janssen CI, Kiliaan AJ (2014) Long-chain polyunsaturated fatty acids (LC-PUFA) from
545 genesis to senescence: the influence of LC-PUFA on neural development, aging,
546 and neurodegeneration. *Prog Lipid Res* 53 (53): 1-17.

547 Jo Y, Lee PCW, Sguigna PV, Debose-Boyd RA (2011) Sterol-induced degradation of
548 HMG CoA reductase depends on interplay of two insigs and two ubiquitin ligases,
549 gp78 and trc8. *P Natl Acad Sci* 108(51): 20503-20508.

550 König B, Koch A, Spielmann J, Hilgenfeld C, Hirche F, Stangl GI, Eder K (2009)
551 Activation of ppar α and ppar γ reduces triacylglycerol synthesis in rat hepatoma
552 cells by reduction of nuclear srebp-1. Eur J Pharmacol 605(1): 23-30.

553 Lee PC, Sever N, Deboseboyd RA (2005) Isolation of sterol-resistant Chinese hamster
554 ovary cells with genetic deficiencies in both insig-1 and insig-2. J Biol Chem
555 280(26): 25242.

556 Li YY, Monroig Ó, Zhang L, Wang SQ, Zheng XZ, Dick JR, You CH, Tocher DR (2010)
557 Vertebrate fatty acyl desaturase with $\Delta 4$ activity. P Natl Acad Sci USA 107(39):
558 16840-16845.

559 Liu Y, Zhang QH, Dong YW, You CH, Wang SQ, Li YQ, Li YY (2017) Establishment
560 of a hepatocyte line for studying biosynthesis of long-chain polyunsaturated fatty
561 acids from a marine teleost, the white-spotted spinefoot *Siganus canaliculatus*. J
562 Fish Biol 91(2): 603-616.

563 Livak KJ, Schmittgen TD (2012) Analysis of Relative Gene Expression Data Using
564 Real-Time Quantitative PCR and the $2^{-\Delta\Delta CT}$ Method. Methods 25: 402-408.

565 Minghetti M, Leaver MJ, Tocher DR (2011) Transcriptional control mechanisms of
566 genes of lipid and fatty acid metabolism in the Atlantic salmon (*Salmo salar* L.)
567 established cell line, SHK-1. Biochim Biophys Acta 1811: 194-202.

568 Monroig Ó, Kabeya N (2018) Desaturases and elongases involved in polyunsaturated
569 fatty acid biosynthesis in aquatic invertebrates: a comprehensive review. Fisheries
570 Sci 84(6): 911-928.

571 Monroig Ó, Wang SQ, Zhang L, You CH, Tocher DR, Li YY (2012) Elongation of long-
572 chain fatty acids in rabbitfish *siganus canaliculatus*: cloning, functional
573 characterisation and tissue distribution of elovl5- and elovl4-like elongases.
574 Aquaculture 350: 63-70.

575 Najafi-Shoushtari SH, Kristo F, Li Y, Shioda T, Cohen DE, Gerszten RE, Naar AM
576 (2010) MicroRNA-33 and the srebp host genes cooperate to control cholesterol
577 homeostasis. Science 328(5985): 1566-1569.

578 Nara TY, He WS, Tang C, Clarke SD, Nakamura MT (2002) The e-box like sterol

579 regulatory element mediates the suppression of human Δ -6 desaturase gene by
580 highly unsaturated fatty acids. *Biochem Biophys Res Commun* 296(1): 111-117.

581 Pillai RS, Bhattacharyya SN, Artus CG, Zoller T, Cougot N, Basyuk E, Bertrand E,
582 Filipowicz W (2005) Inhibition of translational initiation by Let-7 MicroRNA in
583 human cells. *Science* 309 (5740): 1573-76.

584 Qin Y, Dalen KT, Gustafsson JA, Nebb HI (2009) Regulation of hepatic fatty acid
585 elongase 5 by LXR α -SREBP-1c. *Biochim Biophys Acta* 1791(2): 140-147.

586 Radhakrishnan A, Ikeda Y, Kwon HJ, Brown MS, Goldstein JL (2007) Sterol-regulated
587 transport of srebps from endoplasmic reticulum to golgi: oxysterols block transport
588 by binding to insig. *PNAS* 104(16): 6511-6518.

589 Rayner KJ, Suárez Y, Dávalos A, Parathath S, Fitzgerald ML, Tamehiro N, Fisher EA,
590 Moore KJ, Fernandez-Hernando C (2010) miR-33 contributes to the regulation of
591 cholesterol homeostasis. *Science* 328(5985): 1570-1573.

592 Sargent JR, Tocher DR, Bell JG (2002) *The Lipids. Fish Nutrition*, (3rd ed.). San Diego,
593 Academic Press 181-257.

594 Shimomura I, Shimano H, Korn BS, Bashmakov Y, Horton JD (1998) Nuclear sterol
595 regulatory element-binding proteins activate genes responsible for the entire
596 program of unsaturated fatty acid biosynthesis in transgenic mouse liver. *J Biol
597 Chem* 273(52): 35299-35306.

598 Siddique BS, Kinoshita S, Wongkarangkana C, Asakawa S, Watabe S (2016) Evolution
599 and Distribution of Teleost myomiRNAs: Functionally Diversified myomiRs in
600 Teleosts. *Mar Biotechnol (NY)* 18(3): 436-447.

601 Škugor A, Slanchev K, Torgersen JS, Tveiten H, Andersen Ø (2014). Conserved
602 mechanisms for germ cell-specific localization of *nanos3* transcripts in teleost
603 species with aquaculture significance. *Mar Biotechnol (NY)* 16(3): 256-264.

604 Tao M, Zhou Y, Li SN, Zhong H, Hu H, Yuan LJ, Luo M, Chen J, Ren L, Luo J, Zhang
605 C, Liu SJ (2018) MicroRNA Alternations in the Testes Related to the Sterility of
606 Triploid Fish. *Mar Biotechnol (NY)* 20(6): 739-749.

607 Tocher DR (2010) Fatty acid requirements in ontogeny of marine and freshwater fish.
608 *Aquaculture Res* 41(5): 717-732.

609 Tocher DR, Bell JG, Dick JR, Crampton VO (2003) Effects of dietary vegetable oil on
610 atlantic salmon hepatocyte fatty acid desaturation and liver fatty acid compositions.
611 Lipids 38(7): 723-732.

612 Xiao YF, Ke Q, Wang SY, Auktor K, Yang Y, Wang GK, Morgan JP, Leaf A (2001)
613 Single point mutations affect fatty acid block of human myocardial sodium channel
614 alpha subunit Na⁺ channels. P Natl Acad Sci USA 98 (6): 3606-3611.

615 Xu P, Vernooy SY, Guo M, Hay BA (2003) The drosophila microRNA miR-14
616 suppresses cell death and is required for normal fat metabolism. Curr Biol 13(9):
617 790-795.

618 Yabe D, Komuro R, Liang G, Goldstein JL, Brown MS (2003) Liver-specific mRNA
619 for insig-2 down-regulated by insulin: implications for fatty acid synthesis. P Natl
620 Acad Sci USA 100(6): 3155-3160.

621 Yang T, Espenshade PJ, Wright ME, Yabe D, Gong Y, Aebersold R, Goldstein JL Brown
622 MS (2002) Crucial step in cholesterol homeostasis : sterols promote binding of
623 scap to insig-1, a membrane protein that facilitates retention of srebps in ER. Cell
624 110(4): 489-500.

625 Zhang QH, Xie DZ, Wang SQ, You CH, Monroig Ó, Tocher DR, Li YY (2014) miR-17
626 is involved in the regulation of LC-PUFA biosynthesis in vertebrates: effects on
627 liver expression of a fatty acyl desaturase in the marine teleost *Siganus*
628 *canaliculatus*. BBA-Mol Cell Biol L 1841(7): 934-943.

629 Zhang QH, You CH, Liu F, Zhu WD, Wang SQ, Xie DZ, Monroig Ó, Tocher DR, Li
630 YY (2016a) Cloning and characterization of lxr and srebp1, and their potential roles
631 in regulation of LC-PUFA biosynthesis in rabbitfishsiganus canaliculatus. Lipids
632 51(9): 1051-1063.

633 Zhang QH, You CH, Wang SQ, Dong YW, Monroig Ó, Tocher DR, Li YY (2016b) The
634 miR-33 gene is identified in a marine teleost: a potential role in regulation of LC-
635 PUFA biosynthesis in *Siganus canaliculatus*. Scientific Reports 6: 32909.

636 Zheng XZ, Leaver MJ, Tocher DR (2009) Long-chain polyunsaturated fatty acid
637 synthesis in fish: comparative analysis of Atlantic salmon (*Salmo salar* L.) and
638 atlantic cod (*Gadus morhua* L.) Δ6 fatty acyl desaturase gene promoters. Comp

639 Biochem Phys B 154(3): 255-263.

640 Zhu X, Chen DX, Hu Y, Wu P, Wang KZ, Zhang JZ, Chu WY, Zhang JS (2015). The

641 microRNA signature in response to nutrient restriction and refeeding in skeletal

642 muscle of Chinese perch (*Siniperca chuatsi*). Mar Biotechnol (NY) 17(2): 180-189.

643

644 **Table 1.** Primers or oligonucleotides used for vector reconstruction or qPCR.

Aim	Gene/Vector name	Primers/Oligonucleotides	Nucleotide sequence
Construction of reporter vectors	pEGFP-miR-33	pEG-pmiR-33-F	CGGA <u>ATTC</u> TAGATAACTGAAGGTATTATTTCAGCTGAGTGGA
		pEG-pmiR-33-R	CGGGATCCTATATAATCAACTTCCACACTAAAG
	PGLO-Insig - 3'UTR	Insig -3'UTR-F	CCCGGGTCTAGAAACTGCTAAGACTATGGCTAATGCTA
		Insig -3'UTR-R	CCCGGGGAGCTCCTTTTACAACACCTGAAACATATCTC
	PGLO-Insig - 3'UTR-MU	Insig -3'UTR-MU-F	CAAGGTTGATGGTAAGGAGAGGGACAGGAA
		Insig-3'UTR-MU-R	TTCCTGTCCCTCTCCTTACCATCAACCTTG
	pmirGLO-R33	pmirGLO-R33-F	CACATGCAATGCAACTACAATGCACCACAGT
		pmirGLO-R33-R	CTAGACTGTGGTGCATTGTAGTTGCATTGCATGTGAGCT
	pcDNA3.1-SREBP	LG-SREBP-F	GCTCTAGAGAAAGATGAATAGCCTGG
		LG-SREBP-R	GGGAAGCTTGCCTAGCTGTTGGTGACC
	pcDNA-Insig1	pcDNA-Insig1-F	CAGGAATTCATGTCCAGACTAGAGGATCA
		pcDNA-Insig1-R	GA <u>ACTCGAG</u> TCAGTCCATGTGGGGCTTCTCGA
QPCR	miR-33	qPCR-miR-33	CGTGCATTGTAGTTGCATTG
		$\Delta 6\Delta 5 fads2$ -F	TCACTGGAACCTGCCCACAT
	$\Delta 6\Delta 5 fads2$	$\Delta 6\Delta 5 fads2$ -R	TTCATTCTCAGACAGTGCAAACAG
		<i>elovl5</i> -F	GCACTCACCGTTGTGTATCT
	<i>elovl5</i>	<i>elovl5</i> -R	GCAGAGCCAAGCTCATAGAA
		Insig -1-F	AGTTACGCCGCCTGAGAAGA
	<i>insig1</i>	Insig -1-R	TGGGCATCACCCTGCTTTC
		Srebp1 -F	CGGAGCCAAGACAGAGGAGTG
	<i>srebp1</i>	Srebp1 -R	GTCTCCCAGCTTCTCCAAGGTAC
		18S-F	CGCCGAGAAGACGATCAAAC
	18S	18S-R	TGATCCTTCCGCAGGTTAC

645 Notes: The underscore in the table indicates the restriction site in primers.

646 **Table 2.** Fatty acid composition (% total fatty acid) in rabbitfish hepatocytes transfected with
 647 miR-33 mimics and negative control (NC) mimics

Fatty acids composition	Treatments	
	NC	miR-33 Mimic
C14:0	0.45±0.13	0.55±0.06
C16:0	8.89±0.77	10.49±0.79
C18:0	7.11±1.07	9.05±0.81
C18:1n-9	12.52±1.08	13.79±1.81
C18:2n-6	2.22±0.16	2.49±0.34
C18:3n-6	0.73±0.05	0.73±0.21
C18:3n-3	0.54±0.07	0.39±0.02
C18:4n-3	0.49±0.02	0.56±0.05
C20:2n-6	0.78±0.13	0.78±0.13
C20:4n-6(ARA)	2.24±0.43	2.70±0.48
C20:3n-3	0.31±0.07	0.33±0.02
C20:5n-3(EPA)	1.69±0.11	1.72±0.25
C22:4n-6	0.26±0.02	0.29±0.06
C22:5n-3	1.75±0.26	1.95±0.36
C22:6n-3(DHA)	7.11±0.94	7.76±1.23
Σ SFA	16.45±1.83	20.08±1.60
Σ MUFA	12.52±1.08	13.79±1.81
Σ LC-PUFA	13.36±1.79	14.75±2.18
C18:4n-3/C18:3n-3 ($\Delta 6\Delta 5$ Fads2)	0.94±0.09 ^a	1.42±0.01 ^b
C22:5n-3/C20:5n-3 (Elovl5)	1.00±0.06	1.12±0.09

648 Notes: Data are means ± SEM (n = 3), different superscript letters at the same line represent higher
 649 significance to each other ($P < 0.05$; t-test). SFA: saturated fatty acids; MUFA: monounsaturated
 650 fatty acid; LC-PUFA: long-chain polyunsaturated fatty acid.

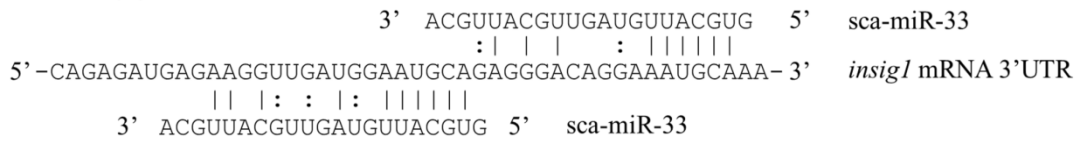
651

652 **Figures**

653 **Fig. 1**

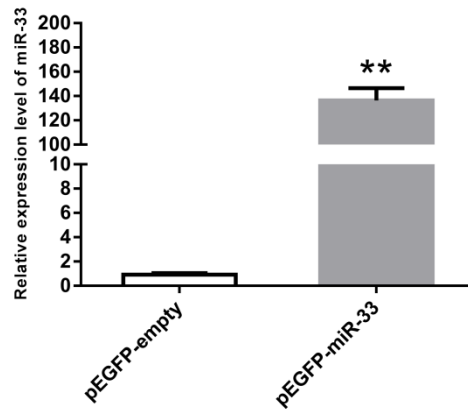
654

655 **(a)**



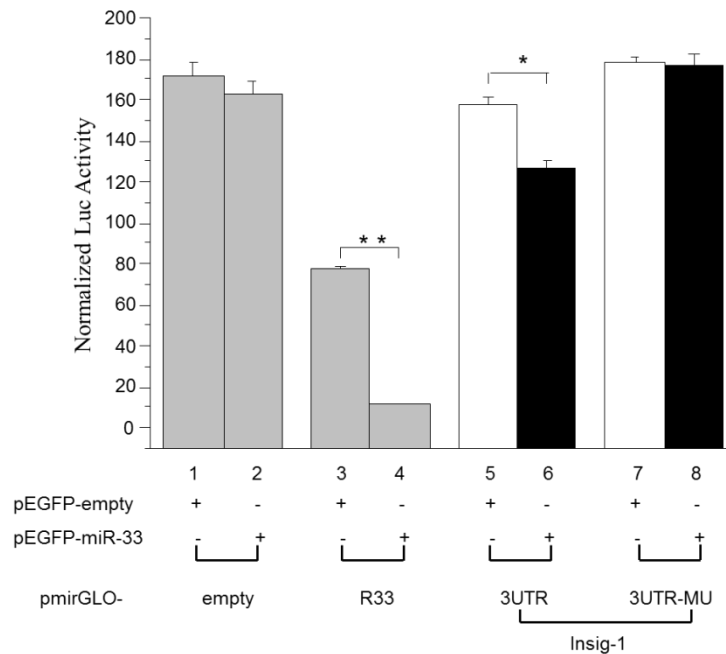
656

657 **(b)**



658

659 **(c)**



660

661 **Fig. 1 (a)** Scheme of miR-33 base pairing the 3'UTR of the rabbitfish *insig1*.

662 33 is over-expressed in HEK 293T cells by transfecting with pEGFP-miR-33.

663 (c) Luciferase activity in HEK 293T cells co-transfected with pEGFP-miR-33 or pEGFP-empty with different recombinant

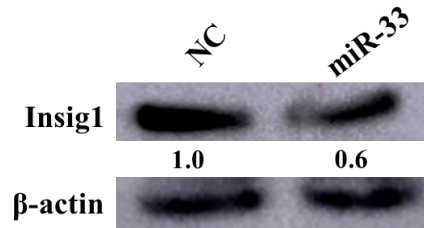
664 dual luciferase reporter vectors: pmirGLO-empty as negative control (lanes 1-2); pmirGLO-R33 as

665 positive control (lanes 3-4); pmirGLO-Insig-3'UTR containing 3'UTR of *insig1* (lanes 5-6);
 666 pmirGLO-Insig-3'UTR-MU with 4 nt site-directed mutation in 3'UTR of *insig1* (lanes 7-8). The
 667 Renilla luciferase activity was used to normalize that of firefly luciferase. Data are shown as means
 668 \pm SEM (n = 8) and asterisks represent significant differences (* P < 0.05; ** P < 0.01; t-test)

669

670 **Fig. 2**

671



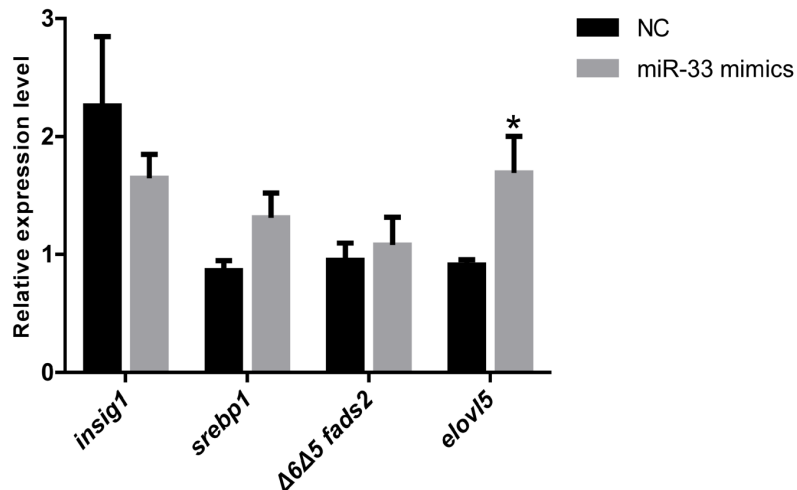
672

673

674 **Fig. 2** miR-33 is a negative regulator of rabbitfish Insig1 at the protein level. The SCHL cells were
 675 transfected with miR-33 or NC mimics, western blotting detected protein expression levels of Insig1
 676 and normalized by Actin. The numbers on the graph refer to the grey value ratio of the target gene
 677 to the reference gene, and the value indicated the relative expression level of the protein.

678

679 **Fig. 3**



680

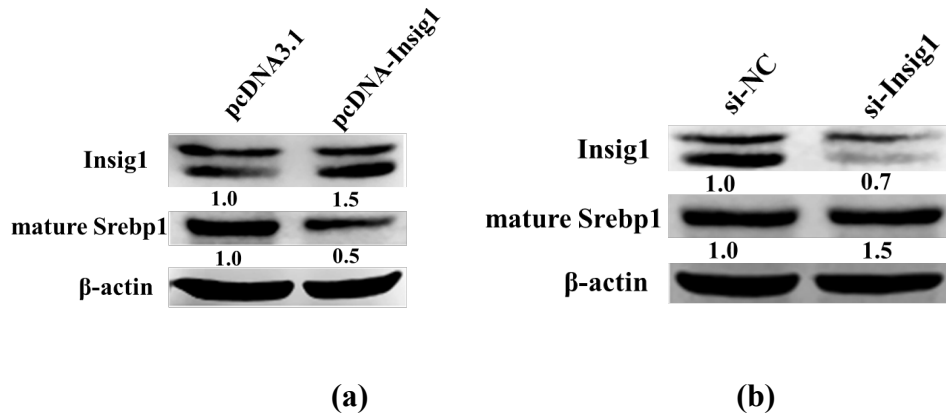
681

682 **Fig. 3** Effects of miR-33 overexpression on the mRNA level of *insig1*, *srebp1*, $\Delta 6\Delta 5$ *fads2* and
 683 *elovl5* in SCHL cells. The gene expression was determined by qPCR in SCHL cells transfected with
 684 miR-33 mimics or NC mimics for 24 h. Data are means \pm SEM (n = 6). Asterisks represent
 685 significant differences (P < 0.05; ANOVA, Tukey's test)

686

687 **Fig. 4**

688



689

690

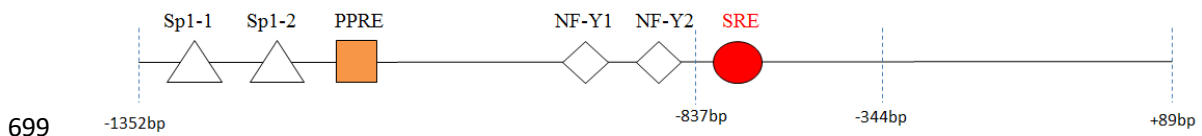
691

692 **Fig. 4 (a)** Effects of *insig1* overexpression on the protein level of Insig1 and Srebp1. **(b)** Effects of
 693 *insig1* inhibition on the protein level of Insig1 and Srebp1. The numbers on the graph refer to the
 694 grey value ratio of the target gene to the reference gene, and the value indicated the relative
 695 expression level of the protein.

696

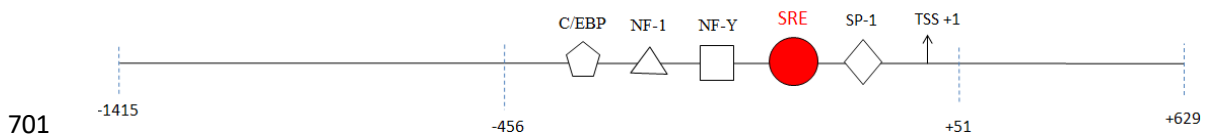
697 **Fig. 5**

698 **(a)**



699

700 **(b)**

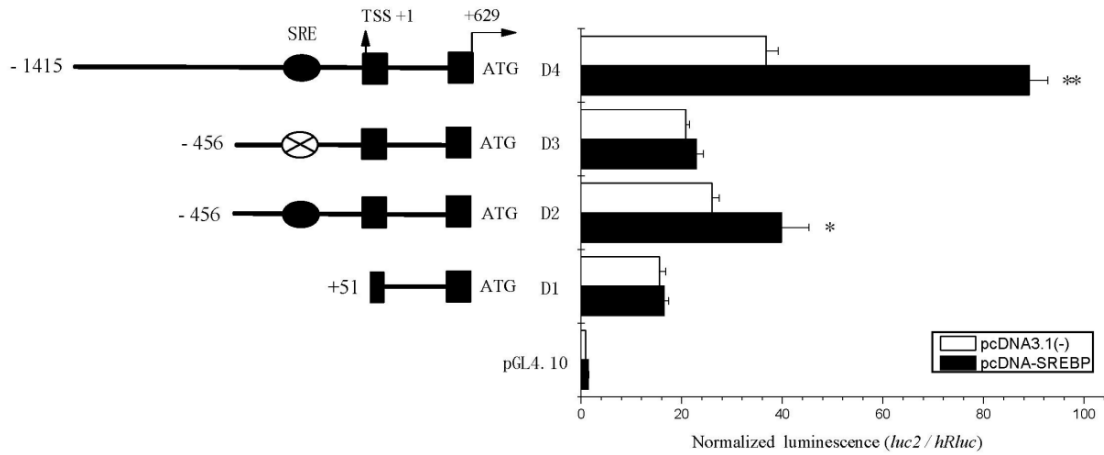


701

702 **Fig. 5** Bioinformatics predicted the binding elements of the upstream promoter sequence of *elov15*
 703 **(a)** and *Δ6Δ5 fads2* **(b)**, where SRE was the acting element of *srebp1*

704

705 **Fig. 6**

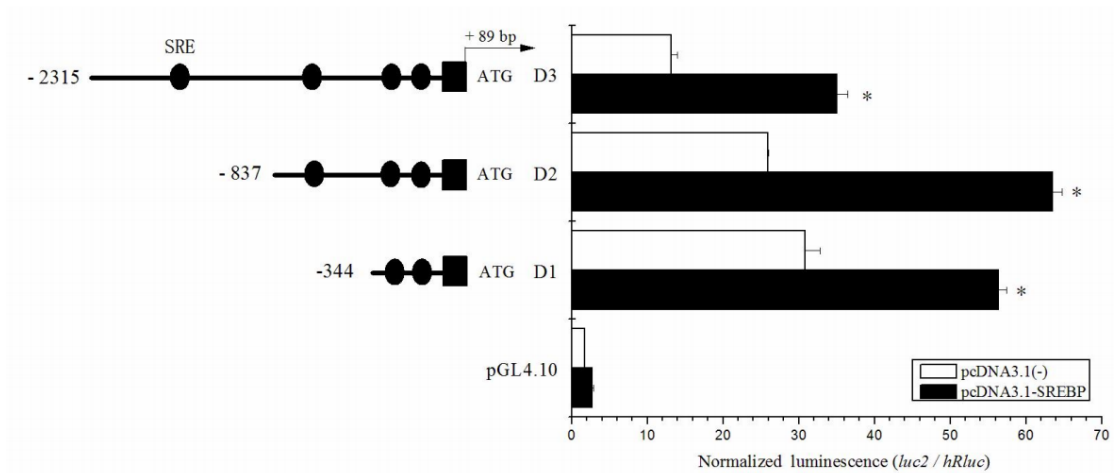


706

707 **Fig. 6** Effects of *srebp1* over-expression on activity of $\Delta 6\Delta 5$ *fads2* promoter deletion. Here is a dual-
 708 luciferase report experiment in HEK 293T cells, with 0.04 ng pGL4.75 plasmid as the internal
 709 reference, and pGL4.10 as the negative control. The black ellipse in the figure represents the position
 710 of the SRE element predicted on the promoter sequence. Data are shown as means \pm SEM and
 711 asterisks represent significant differences (* $P < 0.05$; ** $P < 0.01$; t-test)

712

713 **Fig. 7**

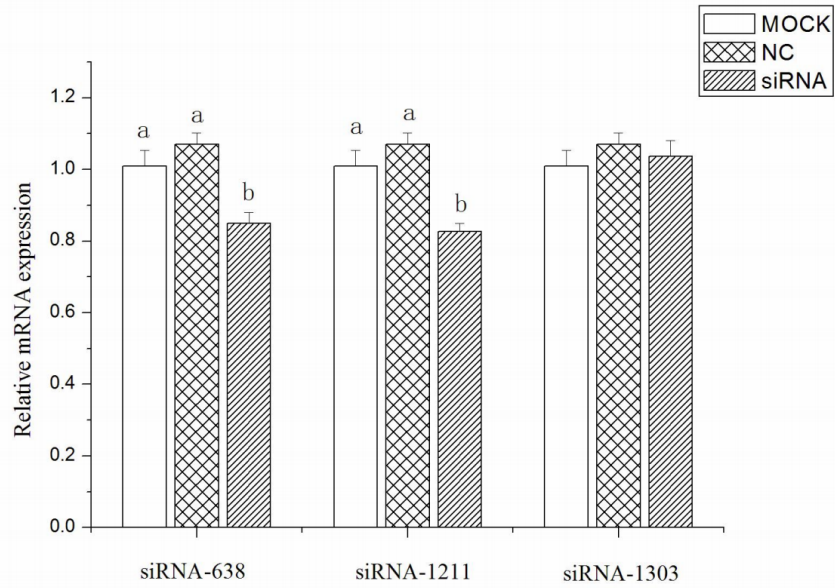


714

715 **Fig. 7** Effects of *srebp1* over-expression on activity of *elov15* promoter deletion. Here is a dual-
 716 luciferase report experiment in HEK 293T cells, with 0.04 ng pGL4.75 plasmid as the internal
 717 reference, and pGL4.10 as the negative control. The black ellipse in the figure represents the position
 718 of the SRE element predicted on the promoter sequence. Data are shown as means \pm SEM and
 719 asterisks represent significant differences (* $P < 0.05$; ** $P < 0.01$; t-test)

720

721 **Fig. 8**



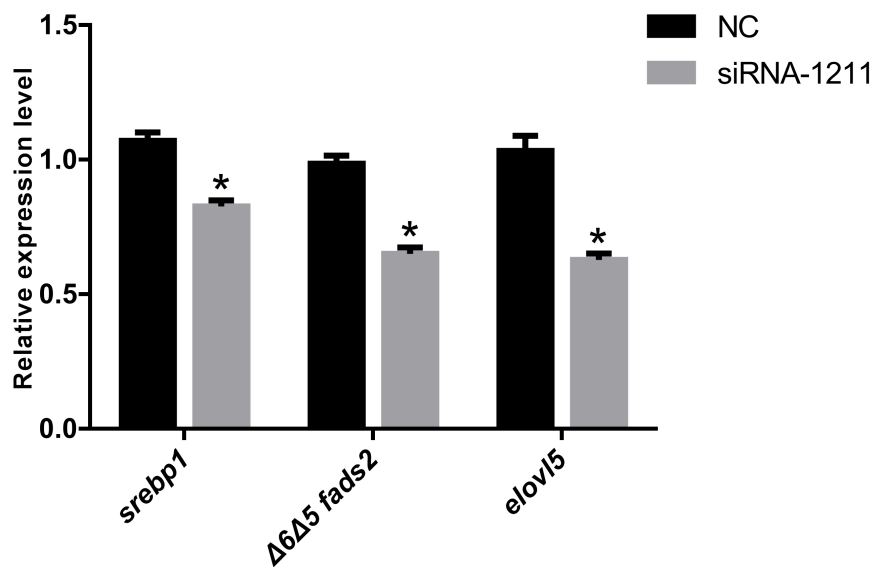
722

723 **Fig. 8** Relative expression of *srebp1* after silenced by different siRNAs. Mock means adding only
 724 transfection reagent groups; NC means adding siRNA negative control group; SiRNA was the
 725 experimental group. Data are means \pm SEM (n = 3) and different superscripts indicate significant
 726 differences ($P < 0.05$)

727

728 **Fig. 9**

729



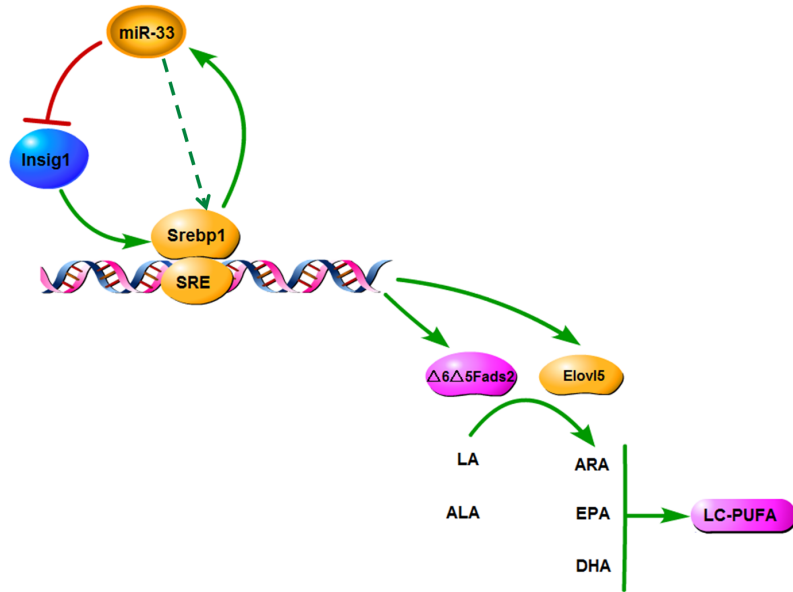
730

731 **Fig. 9** Relative expression of *srebp1*, $\Delta 6\Delta 5$ *fads2*, *elovl5* gene after silenced by siRNA-1211 in
 732 SCHL cells. NC means adding siRNA negative control group; SiRNA-1211 was the experimental
 733 group. Data are means \pm SEM (n = 3) and asterisks represent significant differences ($P < 0.05$;
 734 ANOVA, Tukey's test)

735

736 **Fig.10**

737



738

739 **Fig. 10** Diagrammatic representation of the roles of miR-33 in regulation of LC-PUFA biosynthesis.

740 The putative mechanism diagram is proposed for effects of miR-33 overexpression on target genes,

741 host genes and LC-PUFA biosynthesis related genes. Red arrows denote suppression; green arrows

742 indicate promotion

743